HIGH-FIDELITY MODELLING AND DYNAMIC ANALYSIS OF DAMAGED TAPERED COMPOSITE STRUCTURES

Erasmo Carrera[#], Andrea Viglietti[†], Enrico Zappino[*]

Politecnico di Torino
Department of Mechanical and Aerospace Engineering
Corso Duca degli Abruzzi, 24
10129, Torino, Italy

[#]e-mail: erasmo.carrera@polito.it, web page: http://www.mul2.com

[†]e-mail: andrea.viglietti@polito.it, web page: http://www.mul2.com

[*]e-mail: enrico.zappino@polito.it, web page: http://www.mul2.com

Keywords: CUF, 1-D model, High-fidelity, Tapered beam, Damaged structures.

ABSTRACT

The analysis of the effects due to a failure of a structural component is of primary interest in the design of aerospace structures. The damages in a structure affect the displacement and stress fields, and the dynamic response can be strongly afflicted too. Free-vibration analyses are performed by an advanced 1-D model to evaluate the modal behavior in a multi-component damaged structure. The present 1-D model, using expansions to evaluate the displacement field over the cross-section, is able to describe complex geometries without approximations. Moreover, it can modify the material proprieties, then the stiffness, at the local level. In this way, a high fidelity description of a damaged structure can be achieved. The results show the capability of the present model to deal with this topic making him a good candidate for a design processing tool.

1 INTRODUCTION

To satisfy the weight requirements, the aircraft structures are composed of several components that distribute the high loads which they undergo. Always more often, many components, such as the skin or the webs, are made of composite material in order to increase the weight saving.

It is clear that, once a component fails, the load is redistributed on the other structural elements and its behavior changes according to the entity of the damage. In the design process, the knowledge of the behavior with the presence of damage is of primary importance. Moreover, the aircraft structures usually have particular shapes to ensure the aerodynamic characteristics. The structures can be tapered or can have a twist angle, features that influence the behavior too. In this work, the tapered shape is considered. In this way, considering the beam elements coincident with the y-axis, the bending stiffness EI(y) changes along the axis. The classical approximation introduced to deal with these geometries is a step-by-step approach that concerns the subdivision of the structure into several rigidly prismatic beams with different cross-sections. The approximation is improved by the increase of the subdivisions. After the introduction of the Finite Element Methods, other works [1][2] have been added to existing analytical methods [3][4].

The presence of damage affects the natural vibrations of the structure, and these alterations can be used to detect structural damage and to understand if the new damaged condition is suitable or not. Several works on the damage detection based on the dynamic behavior have been proposed. Based on the FEM method, the works of Wang [5], Nguyen [6] and Pollayi and Yu [7] can be found. On the contrary Pèrez et al. [8] performed extensive experimental analyses on the vibration of damaged laminates.

The classical theories can be not suitable to deal with damaged structures, and models with 3-D-like capability are required.

Carrera et. al [9] used a beam model based on the Carrera Unified Formulation (CUF) to analyze damaged aircraft structures.

In the 1-D CUF models, the displacement field over the cross-section is described through expansion functions. In this way, no geometrical approximations are introduced in the problem, and the model can deal with arbitrary geometries, material, and boundary conditions. After the first class of models based on Taylor expansions (TE model), the Lagrange polynomials have been introduced. In this model, each component can be modeled using ad-hoc formulation (Component-Wise approach). Works about this topic and its capability in the aerospace field are [10][11].

Carrera et al. [9], using the CW approach, have analysed different prismatic structures made of an isotropic material introducing different damage cases. For each case, the frequencies have been evaluated, and the modal shapes have been compared using the MAC (Modal Assurance Criterion)[12]. This criterion has already been used in the analyses of damaged bridges by Salawu and Williams [13].

This work presents a 1-D CUF model used to analyse tapered aircraft structures affected by different damage cases. After an explanation of the mathematical method used in this work, the results obtained from a simple reinforced structure and a complex wing structure are provided. Finally, some leading remarks are drawn.

2 REFINED BEAM MODEL

In this section, the 1-D Carrera Unified Formulation is rapidly explained. For more details about these formulations and their capability, the book [14] is suggested.
After the first part about some preliminaries, the present formulation is explained, and the section will be concluded with the approach used to introduce the damage.

2.1 Preliminaries

In this work, two different frames are used to describe the geometries and the FEM models. The first frame (X_G, Y_G, Z_G) is the global coordinate system of the 3-D space. In this space, different BEAMs are rotated and translated to create a complex structure. The second frame (x, y, z) defines the beam element respect the global reference system. The axis y identifies the beam axis and the plane (x,y) identifies the cross-section. The global frame is shown in the figure 1*a* that is the first case studied.

The displacement field of a generic point can be defined as the vector **u**

$$\boldsymbol{u}(x,y,z)=\{u_x\ u_y\ u_z\}^T \tag{1}$$

The following linear strain-displacement relation can obtain the strain vector composed by six components:

$$\boldsymbol{\varepsilon}=\boldsymbol{b}\boldsymbol{u}(x,y,z) \tag{2}$$

where $\boldsymbol{b}$ is a differential operator (6x3 matrix). The stress is derived from the Hook's law through the following form

$$\boldsymbol{\sigma}=\boldsymbol{C}\,\boldsymbol{\varepsilon} \tag{3}$$

where **C** is the 6x6 *material stiffness matrix*. It contains the elastic coefficients. An explanation about this matrix for the isotropic material and also for the orthotropic material can be found in [15] and [16]. The explicit formulations of the matrix $\boldsymbol{b}$, of the strain vector and the stress vector, can be found in the book by Carrera *et al*. [14].

2.2 One-dimensional model via CUF

The *Carrera Unified Formulation* expresses the displacement field **u** as

$$\boldsymbol{u} = F_\tau(x, z)\,\boldsymbol{u}_\tau(y) \qquad \tau=1,2,\ldots..,M. \tag{4}$$

where $\boldsymbol{u}_\tau$ is the displacement vector. F_τ represents an expansion used to describe the displacement field over the beam cross-section. M is the number of terms of the expansion.

Several works using the Taylor-like expansion polynomials as F_τ have been presented. Considering the TE model (TE: Taylor expansion) of the first order, the displacement field of the term u_x for example, is expressed as follow:

$$u_x = u_{x1} + xu_{x2} + zu_{x3} \tag{5}$$

The TE models can be deepened in [17].

The LE models represent another more powerful 1-D CUF model. In this class, the Lagrange expansions are used. They are expressed by an isoparametric formulation and can deal with any geometrical shape. In these models, the introduced unknowns are only translational displacements.

Several Lagrange polynomial sets exist, and the nine-point elements (L9) are used in this work. Other types of polynomials sets are the four-point elements (L4). More details and the interpolation functions can be found in [18]. To improve the approximation, the use of more Lagrange elements to describe the cross-section is suggested.

Figure 1c shows an example of the Lagrange description used in the first analysed structure of this work.

2.3 FEM Solution

The Finite Element theory is implemented to solve the problem.

The shape functions N_i are introduced to approximate the displacement of the beam axis and then the vector $\boldsymbol{u}$ can be written as

$$\boldsymbol{u}(x,y,z) = F_\tau(x, z)\, N_i(y)\boldsymbol{q}_{\tau i} \tag{6}$$

where $\boldsymbol{q}_{\tau i}$ is the nodal displacements vector.

Through the PVD (Principle of Virtual Displacements), shown in 7, the stiffness matrix (from δL_{int}) and the mass matrix (from δL_{ine}) are obtained in terms of Fundamental Nucleus (FN), a 3x3 matrix.

$$\delta L_{int} = -\delta L_{ine} \tag{7}$$

The expressions of the FN terms are shown in [9] and an exhaustive description about the derivation of the FN is presented in [14].

By substituting the terms of the FN into the PVD, the undamped dynamic problem is obtained as:

$$\boldsymbol{M\ddot{u}+Ku=0} \tag{8}$$

Considering harmonic solutions, the natural frequencies ω_k can be obtained solving the classical eigenvalue problem shown in 9.

$$\boldsymbol{(-\omega_k^2 M+K)u_k=0} \tag{9}$$

where $\boldsymbol{u_k}$ is the k_{th} eigenvector.

2.4 Rotation & Assembly Procedure

Trough the present formulation, different components of a complex structure can be modelled separately and then rotated and translated in the space in order to be joined. The rotation around the three axes of the beam reference frame can be done through a rotation matrix $\boldsymbol{\Lambda}$. In this way a generic displacement $\boldsymbol{u}$ in a local reference system can be rotated in the global reference system through the following formulation:

$$\boldsymbol{u_{GLOB}} = \boldsymbol{\Lambda}\, \boldsymbol{u_{loc}} \tag{10}$$

More details about the rotation matrices can be found in [19].

In the present LE formulation, the structures can be joined very easily because the displacements are the only unknowns. The assembling is done without incurring in issues by imposing the congruence of the displacements in the shared nodes. Figure 1*c* shows the connection of the panel with the stringer in the structure used in this work.

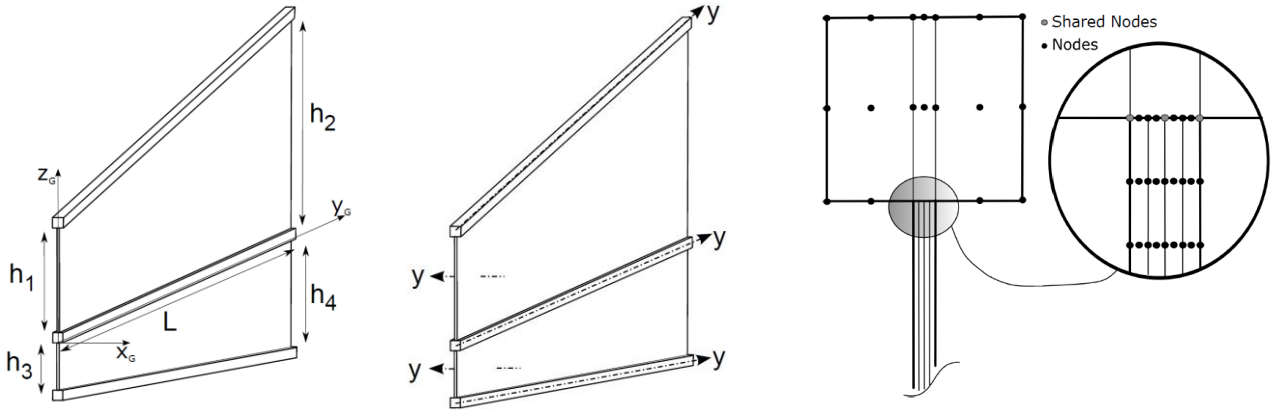

(a) Considered Structure *(b) FEM formulation* *(c) Connection*

Figure 1: Three-stringer spar.

2.5 Damage Description

In this work to describe the damage, a simple damage modelling is adopted. In the damaged zone, the material is degraded according to the formula

$$E_d = d \times E \qquad 0 \leq d \leq 1 \tag{11}$$

where E is Young's modulus. Considering an orthotropic material, the terms E_{22}, E_{33}, G_{12} etc. are degraded in the same way. In this way, the capability of the component to cooperate with the structure is of immediate understanding. In other words, if the parameter $d=1$ is applied to the whole component, the material is not degraded and the component is not damaged.

Thanks to the capability of the present model, the damage can be extended from an area of the beam cross-section to the whole component.

3 3-STRINGER SPAR

The reinforced structure shown in figure 1a is considered. There are two panels with different tapered shapes reinforced by three metallic stringers with a square cross-section. The panels are made of composite material. The laminate has four layers with a lamination of 0°/90°/90°/0°. The present model allows each layer to be described. The material *x*-axis, so the direction of the fiber, coincides with the Y_G axis. The stiffeners are made of an aluminum alloy with an elastic modulus of $E=71.7e^9$ Pa, a Poisson's ratio of 0.3 and a density of 2810 kg/m^3. The panels are made of a laminate of *CFRP: Carbon Fibre Reinforced Polymer*. This composite has the following proprieties: $E_{LL}=50e^9$ Pa, $E_{TT}=E_{ZZ}=10e^9$ Pa, $G=5e^9$ Pa, Poisson's ratio $\nu=0.25$ and density of 1700 kg/m^3.

The dimensions of the structures are $L=2$, $h_1=0.48$, $h_2=0.98$, $h_3=0.2$ and $h_4=0.4$. The dimensions are expressed in meters. The stringers have a square cross-section with an area equal to 0.0016 m^2. The central stiffener is parallel to the Y_G axis. The highest extremity of the structure is clamped.

A Nastran Solution with a high number of degree of freedom is considered as the exact solution. The composite panels are described with solid elements HEX8 where each layer is described by a layer of solid elements. This approach leads to 179700 Dofs.

The LE model uses six B4 elements to describe the stiffeners. One three-node beam element along the thickness of each layer of the laminate is used. Thus, the panel is described with four B3 elements. The model is characterized by 13167 degrees of freedom. The use of the present formulation to describe tapered structure is given in [19].

Figure 2 shows the damage cases considered in this case. Thanks the capability of the present model, the panel is described through a Layer-wise approach. In this way, each panel can be separately individuated. First, an external layer as damaged component is considered (Case 1). Then, an internal one is damaged (Case 2). Figure 2c shows the third studied case. The area near the central stringer is damaged, and the damage involves all the layers of the laminate. Here X_d is equal to $0.8h_2$. At the tip, X_d will be equal to $0.8h_1$.
For each case three different damage levels (DL) are considered: d=0.9, d=0.5 and d=0.1.

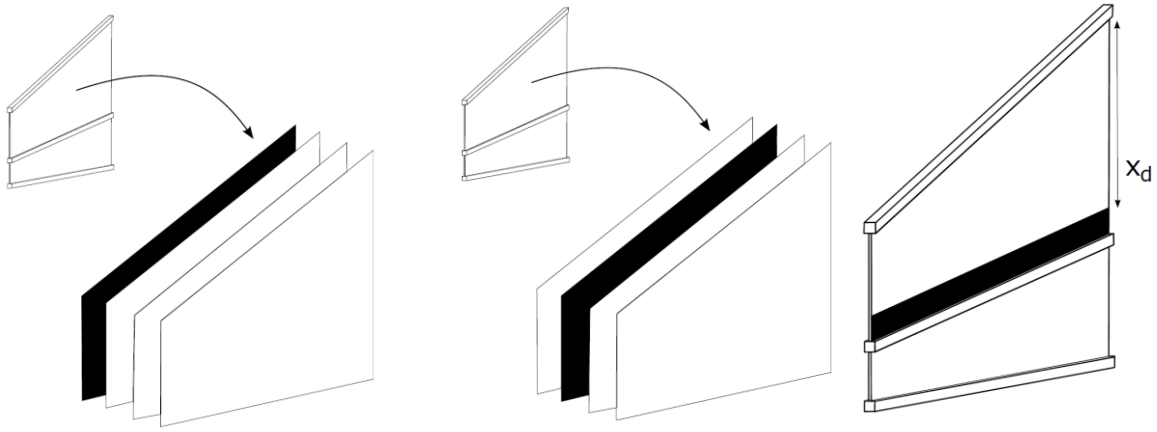

(a) Case 1 *(b) Case 2* *(c) Case 3*

Figure 2 : Considered Damage Cases.

Figure 3 shows the first ten modal shape while Table 1 lists the values of the first 15 frequencies. The first two columns present the values obtained from the Nastran Model and from the current model. There is a good correspondence between the two models with very low errors in most frequencies. The other columns show the results obtained with the three damage cases with the three values of *d*. The histograms shown in figure 4 presents a visual information of the evolution of the first ten frequencies. The considered damage have a weak influence on the first two modes and their frequencies remain about the same. The same behavior can be found in the fourth frequency. The other frequencies, due to their shell-like behavior, are more affected by this type of damage. For a better investigation, this graph has to be analysed also using the MACs shown in figure 5 where the modal shapes of the damaged model are compared with the undamaged ones. MAC values equal to 1 means that the two analysed modal shapes are the same.

From these graphs, the less influence of the damage on the internal layer respect an external one can be noted. In fact, considering a DL of d=0.5 in the case 2, there are no effects on the modal behavior. Moreover, the effects in the case 1 are mainly present at high frequencies. Except for a little variation on the fifth frequency, the first ten modes are not affected in the modal shapes although the frequencies decrease.

In the third case, though the damaged area is smaller respect the entire layer, the proprieties are degraded on all the four layers. In this case, the effects are already identifiable in the first ten modes with only a DL of d=0.5.

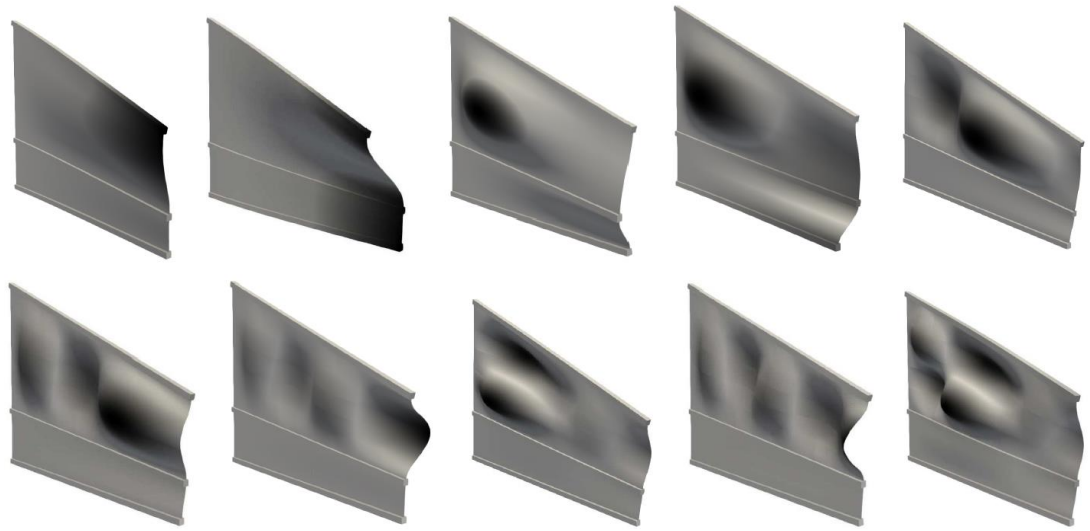

Figure 3: First 10 modes of the three-stringer spar.

	NAS_{SOLID}	LE_{MODEL}	Case 1			Case 2			Case 3		
			d=0,9	d=0,5	d=0,1	d=0,9	d=0,5	d=0,1	d=0,9	d=0,5	d=0,1
f_1	7,14	7,14	7,14	7,12	7,09	7,14	7,13	7,1	7,14	7,09	6,61
f_2	7,96	7,89	7,88	7,84	7,79	7,88	7,85	7,8	7,87	7,8	7,49
f_3	13,58	12,31	12,17	11,29	9,83	12,24	11,85	11,15	12,15	10,92	7,74
f_4	14,53	13,02	12,94	12,75	12,51	12,98	12,85	12,75	12,93	12,73	10,58
f_5	20,49	18,02	17,69	16,1	13,66	17,89	17,28	16,34	17,68	15,82	12,7
f_6	26,62	23,75	23,32	21,15	17,49	23,59	22,77	21,47	23,33	20,88	14,38
f_7	30,26	28,44	27,93	25,51	21,57	8,23	27,23	25,75	27,93	24,99	16,97
f_8	32,99	32,54	32,02	29,58	24,99	32,26	30,87	28,73	31,74	27,76	22,13
f_9	38,43	36,07	35,29	31,34	26,28	35,92	35,2	34,16	35,41	31,6	22,48
f_{10}	42,35	41,33	40,71	37,56	31,17	41,06	39,66	37,4	40,45	35,86	29,64
f_{11}	46,73	46,97	46,92	42,31	32,79	46,95	46,85	46,06	46,93	43,47	30,24
f_{12}	47,8	47,57	47,33	45,87	39,48	47,49	47,11	46,76	47,31	44,65	37,74
f_{13}	50,1	49,62	48,59	46,83	41,45	4948	48,75	47,54	48,87	46,84	40,1
f_{14}	50,85	50,85	49,87	48,16	46,65	49,99	49,76	48,74	49,84	47,37	45,24
f_{15}	54,18	52,98	52,14	50,19	46,67	52,64	52,08	50,05	51,8	50,02	46,77

Table 1: First 15 natural frequencies (Hz) of the three-stringer spar with different damage cases

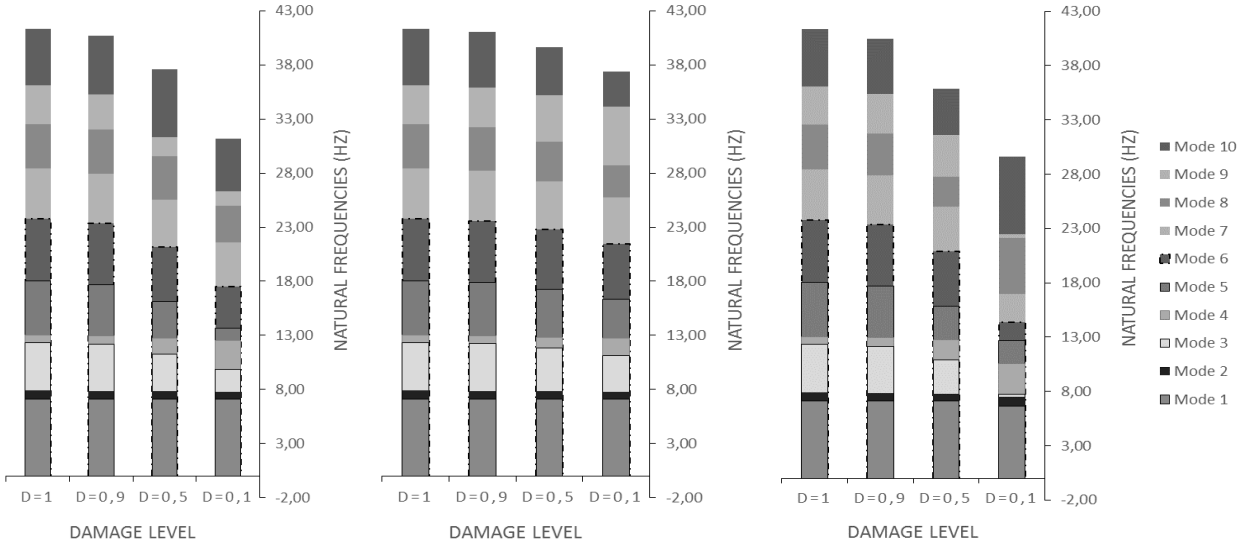

(a) Case 1 *(b) Case 2* *(c) Case 3*

Figure 4: Histograms about the frequencies of the three damage cases.

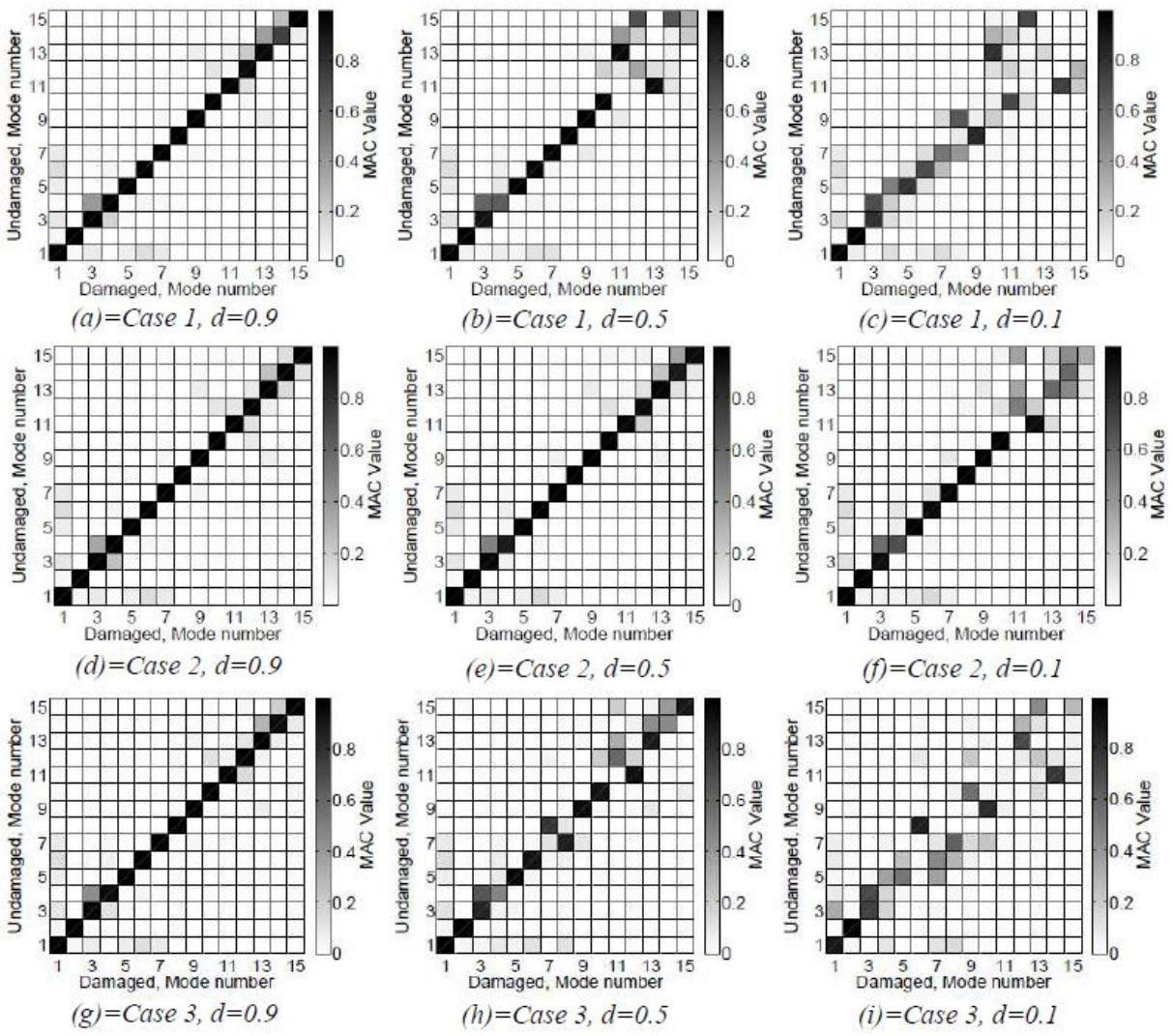

Figure 5: MAC graphs of the 3-stringer spar.

4 COMPLEX WING STRUCTURE

In this section, an example of a complex aeronautic structure is showed. A multi-component tapered wing is considered, and figure 6 shows its geometry. The wing has a length of L=5 m. The tapered shape modifies the chord that changes from a value of R_1=1.48 m to a value of R_2=0.782 m. The wing thickness is constant, and it is equal to H=0.208 m. The spar is composed of two spar caps and the web with the thickness of t_w= 3 mm. The spar caps have dimensions equal to a=8 mm, b=5 mm, c=20 mm and d=45 mm. The spars are made of aluminum alloy with the proprieties before introduced. The skin is a 4-layer laminate made of *CFRP* and it has a thickness of t_s= 4 mm. There are three ribs made of aluminum alloy placed at Y_r=1,6666667 m. Its thickness is equal to t_s. The central spar is aligned with the Y_G axis. For the sake of brevity, the effects of two damage cases on the first bending and first torsional mode are considered. For the result validation, a Nastran solid model with more than 330000 Dofs is used. The LE model uses six 4-node beam elements along the length of the spar-caps and uses one 3-node beam element placed over the thickness to describe the web and each layer of the skin. The same description is used for the ribs. The model has 42682 Degrees of Freedom.

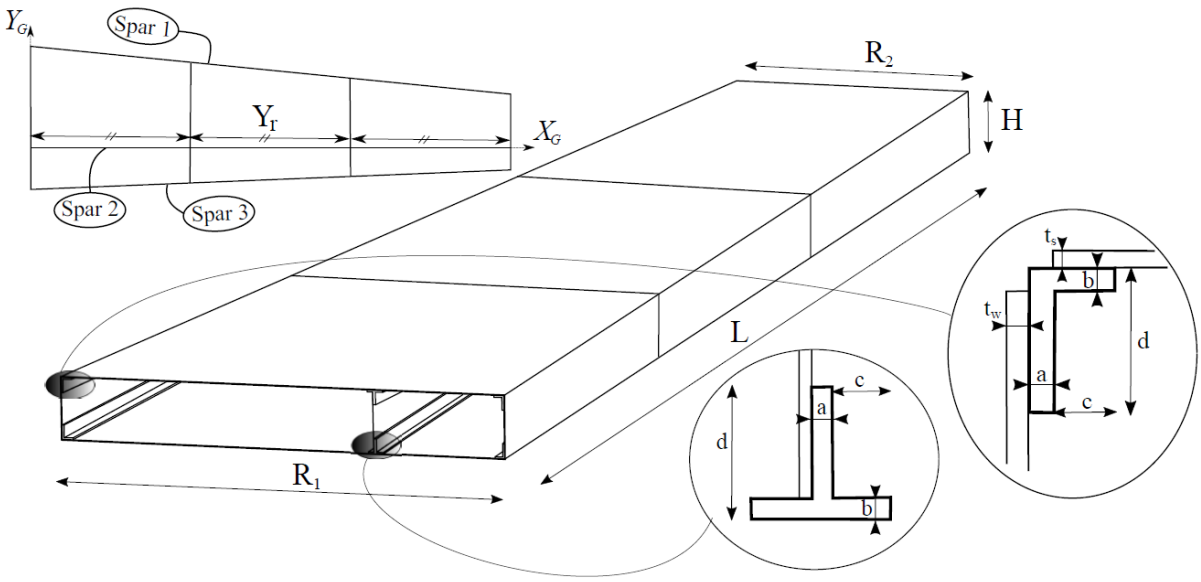

Figure 6: Complex wing structure.

The first case of damage considers only the top spar caps. The second case considers as damaged component the complete spar, so the two spar caps and the web. The condition is implemented for each one of the three spars of the structure, and the damage involves the entire component, from *YG*=0 to *YG*=5 m. The DL is equal to d=0.1. Table 2 shows the frequencies of the two considered modes. The first two columns are the frequencies of the present model compared with those obtained from the Nastran Model. The other six columns are the six damage cases. In the first row there is the case number and in the second row the considered damaged component In the first mode, considering the damage of the spar caps, the decrease of the frequencies are very weak, and the case 2 introduces the largest effect.
On the contrary, the deformations show more details about the behavior. Figures 7 shows the deformation at the tip of the first mode. A damage of the top spar cap in the first spar deletes the torsional effect due to the tapered shape (see figure on the left). On the contrary, the case 3 increases this effect on the deformation. More interesting the case where the whole spar is damaged.

Although the difference in the frequency in the damage cases 4, 5 and 6 is very low, the effects on the deformation are very different (right picture in figure 7). The spar n.2 has a weak effect on the deformation although the frequency has the largest decrease (7%) respect the other two cases. The spar n.1 reverses the torsional effect contrariwise the case 6 increases this behavior (the third spar is damaged).

Figure 8 shows the deformation at the tip of the first torsional mode. Obviously, the damage about the spar cap has less influence respect the whole spar. The largest effects on the frequency can be found if the damage is located in the first spar. Case 1 and Case 4 introduce a decrease of 1.2% and 9.4% in the frequency respectively.

In the first three cases, the deformation at the tip is only influenced by the third case. Here, the torsional effect is increased with largest displacements of the displacements along the z-axis of the first spar, as shown in the picture on the left of figure 8. The picture on the right presents the effects if the whole spar is damaged. Case 4 and Case 6 introduce the most significant alterations in the deformation.

			Damage case					
			Case 1	Case 2	Case 3	Case 4	Case 5	Case 6
	NAS_{SOLID}	LE_{MODEL}	Spar Caps 1	Spar Caps 2	Spar Caps 3	Spar 1	Spar 2	Spar 3
1ST Bending	9,57	9,58	9,35	9,3	9,35	8,96	8,87	9,01
1ST Torsional	38,5	39,4	38,91	39,15	39,18	35,7	37,73	37,67

Table 2: First bending and torsional natural frequencies (Hz) of the wing structure.

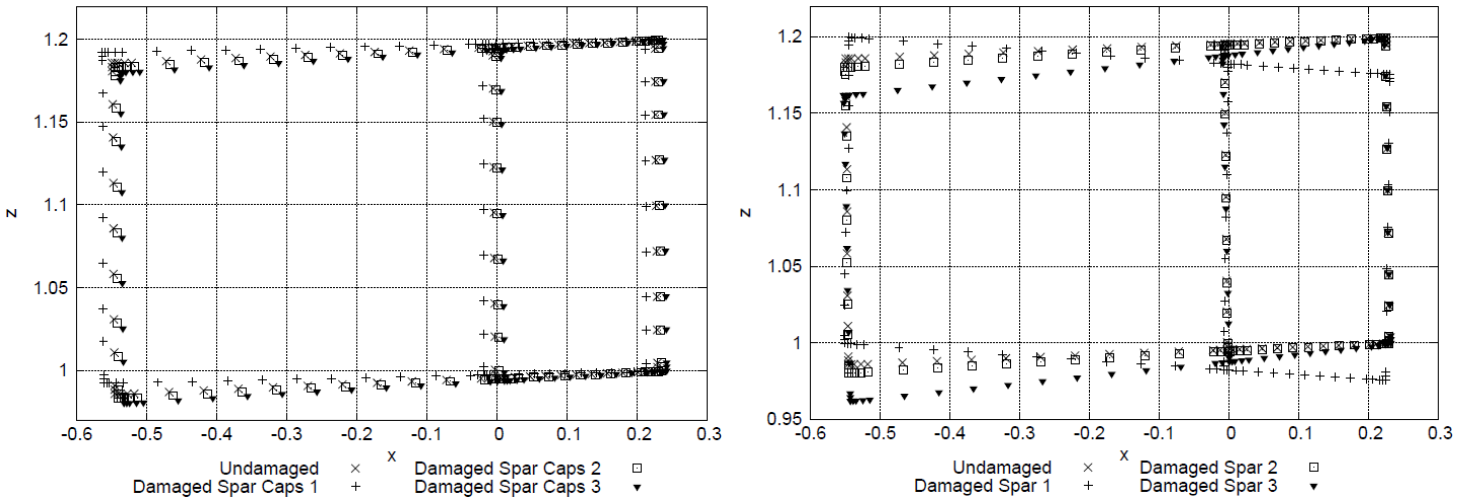

Figure 7: Deformation at the tip in the first bending mode.

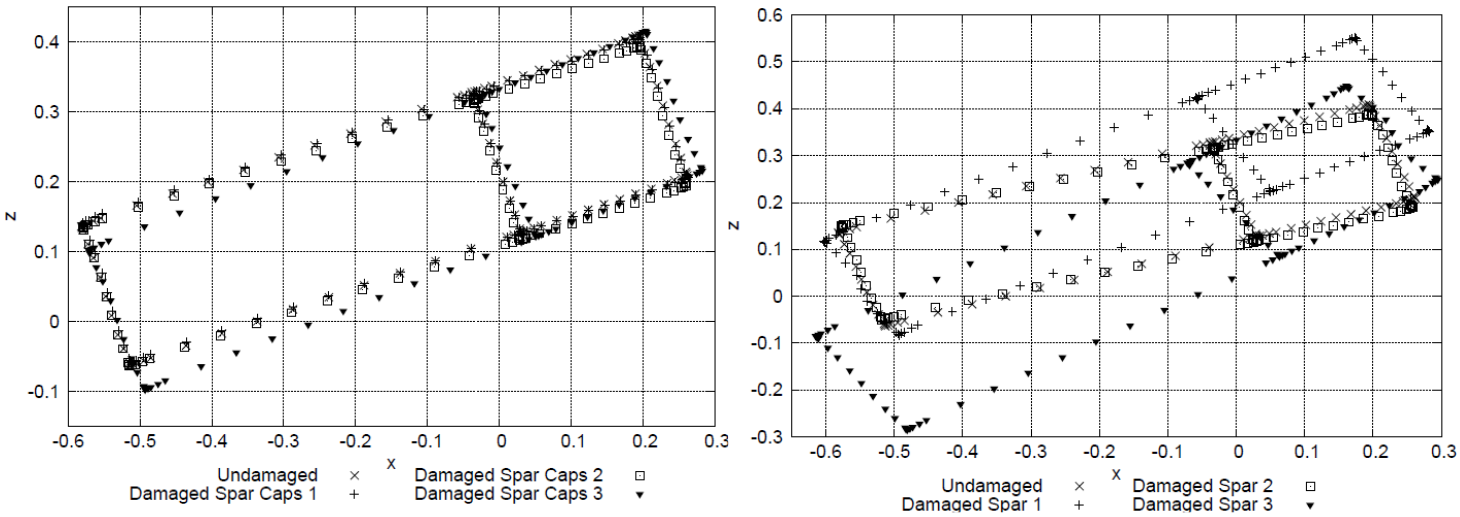

Figure 8: Deformation at the tip in the first torsional mode.

5 CONCLUSION

Using an advanced 1-D model based on the Carrera Unified Formulation, an High-Fidelity description of tapered multicomponent aerospace structures is performed introducing different types of damage. Through free-vibration analyses, the capability of the present model to deal with complex structures made of composite material is investigated also evaluating the alterations in the dynamic behavior due to the presence of damage. The damage is introduced through the degradation of the mechanical proprieties of the material. Aerospace structures are good candidates for this work because of their no-classical geometry and the presence of several components.
Considering the obtained results, the following remarks can be made:

- The present 1-D model is able to describe multicomponent structures without geometrical approximations. In this way, quasi-3D results can be achieved maintaining a great reduction in the computational cost.
- The present model provides the possibility to modify the material proprieties at the local level. Moreover, being able to describe each layer of a laminate, a local and global layer damage can be introduced in the composite material.
- There is the possibility to have damages that affect only the highest frequencies. For this reason, for a damage detection purpose, a model able to detect with accuracy a wide range of frequencies is suggested.
- A damage introduces an alteration in the dynamic behavior that can be suitable or not, depending on the structure functionality. For example, the deformation in an aeronautical structure may not exceed determined values for aerodynamic and aero elastic reasons.

REFERENCES

[1] H.L. Schreyer. Elementary theory in linearly tapered beams. *Journal of the Engineering Mechanics Division*, 104(3):515-527, 1978.
[2] C.J. Brown. Approximate sti_ness matrix for tapered beams. *Journal of Structural Engineering*, 110(12):3050-3055, 1984.
[3] P. Cicala. *Sulle travi di altezza variabile*. Laboratorio di Aeronautica, Tipografia Vincenzo Bona, Turin, Italy, 1939.
[4] S.P. Timoshenko and J.N. Goodier. *Theory of elasticity*. McGraw-Hill, 1970.
[5] Wang, Y., Liang, M., and Xiang, J.. Wind Turbine Blades Based on Dynamics Analysis and Mode Shape Difference Curvature Information *Mechanical Systems and Signal Processing* Vol. 48, 2014, pp. 351367.
[6] Nguyen, K.. Mode Shapes Analysis of a Cracked Beam and Its Application for Crack Detection *Journal of Sound and Vibration* Vol. 333, No. 3, 2014, pp. 848872.
[7] Pollayi, H., and Yu,W.. Modeling Matrix Cracking in Composite Rotor Blades within VABS Framework. *Composite Structures* Vol. 110, 2014, pp. 6276.
[8] Pérez, M., Gil, L., Snchez, M., and Oller, S.. Comparative Experimental Analysis of the Effect Caused by Artificial and Real Induced Damage in Composite Laminates. *Composite Structures* Vol. 112, 2014, pp. 169178.
[9] Carrera E., Pagani A. and Petrolo M.. Free Vibrations of Damaged Aircraft Structuresby Component-Wise Analysis. *AIAA JOURNAL* Vol. 54, No. 10, October 2016.
[10] Carrera, E., Pagani, A., and Petrolo, M.. Component-Wise Method Applied to Vibration of Wing Structures. *Journal of Applied Mechanics* Vol. 80, No. 4, 2013, Paper 041012.
[11] Carrera, E., and Pagani, A.. Accurate Response of Wing Structures to Free-Vibration, Load Factors, and Nonstructural Masses. *AIAA Journal* Vol. 54, No. 1, Jan. 2016, pp.227-241.
[12] Allemang, R. J., and Brown, D. L.. A Correlation Coefficient for Modal Vector Analysis *Proceedings of the International Modal Analysis Conference* 1982, pp. 110116.
[13] Salawu, O., and Williams, C.. Bridge Assessment Using Forced Vibration Testing. *Journal of Structural Engineering* Vol. 121, No. 2, 1995, pp. 161173.
[14] Carrera E., Cinefra M., Petrolo M., and Zappino E.. *Finite Element Analysis of Structure through Unified Formulation* John Wiley & Sons Ltd, 2014.
[15] Tsai, S. W.. *Composites Design, 4th ed* Think Composites, 1988.
[16] Reddy, J. N.. *Mechanics of laminated composite plates and shells. Theory and Analysis, 2nd ed.* CRC Press, 2004.
[17] Carrera, E., Giunta, G., and Petrolo, M.. *Beam Structures: Classical and Advanced Theories* Wiley, Hoboken, NJ, 2011.
[18] Carrera E., Pagani A. and Petrolo M.. Classical, Refined, and Component-Wise Analysis of Reinforced-Shell Wing Structures. AIAA JOURNAL Vol. 51, No. 5, May 2013.
[19] Zappino, E., Viglietti, A., and Carrera, E.. The analysis of tapered structures using a component-wise approach based on refined one-dimensional models. *Aerospace Science and Technology* Vol. 65, June 2017, Pages 141-156